3E4. NLR 7301 SUPERCRITICAL AIRFOIL OSCILLATORY PITCHING AND OSCILLATING FLAP

R.J. Zwaan, NLR

INTRODUCTION

The supercritical airfoil NLR 7301 has a maximum thickness of 16.5 per cent of the chord. In the Set of two-dimensional aeroelastic configurations this airfoil represents the category of thick and blunt-nosed airfoils.

The airfoil was investigated in two windÄtunnel tests with different models. In the first test the model could be driven harmonically in a pitching motion about an axis at 40 per cent of the chord. Information about this configuration is designated with the letter "A". In the second test harmonic rotation of a trailing-edge flap was considered. The flap axis was located at 75 per cent of the chord; the flap had no aerodynamic balance. Information about this configuration is designated with the letter "B".

In transonic flow the contribution of the shock to the aerodynamic loading can of course be very different. As an illustration, pressure distributions on the upper surface are compared for a flow with a strong shock and a shock-free flow. Also results of thin-airfoil theory have been added. In the strong shock cases (A: Fig. 1, B: Fig. 5) the pressure peak due to the moving shock dominates in the pressure distribution, with a strength which diminishes with frequency. Although the flow conditions are the same for both configurations, the mean pressure distributions differ slightly. The cause of these differences could not be traced. In the shock-free cases (A: Fig. 2, B: Fig. 6) the pressure distribution shows a wide bulge. The pressure distributions of configuration A show very clearly that with increasing frequency the bulge decreases while at the same time a weak shock develops. Also here the mean pressure distributions should be the same. For unexplained reasons, however, shock-free flow could only be realized at slightly different Mach numbers.

Lift and moment coefficients are presented in figures 3 and 4 for configuration A and in figures 7 and 8 for configuration B. The influence of fixing boundary layer transition is remarkable. Configuration A shows only minor differences. Forced transition at 0.3c is obviously not so effective in this case. The differences are larger for configuration B, which includes also fixed transition at 0.07c. Characteristic changes occur in particular in the lift coefficient at low frequencies. Transition fixing has obviously the effect of reducing both the lift magnitude and the phase lag.

An aspect that emerges especially in the present case of a supercritical airfoil is the difference in the specification of theoretical and experimental shockÄfree flow. In the General Review it was pointed out that this difference is mainly due to viscous effects and tunnel interference. It was further proposed to choose the CT specification such that theory would produce a flow similar to that observed in the experiment. This is illustrated in figure 9 where the theoretical design pressure distribution calculated with a hodograph theory is compared with a shockÄfree pressure distribution measured at free transition.

LIST OF SYMBOLS AND DEFINITIONS

ALPHA	mean wing incidence, α_m, deg
AMPL	flap amplitude, δ_0 deg; see note below
C2	pitch amplitude, α_0, deg; see note below
CL	mean wing lift coefficient, C_L
CLIM	k_α" in Tables 5 to 14; k_c" in Tables 15 to 23
CLRE	k_α' in Tables 5 to 14; k_c' in Tables 15 to 23
CM	mean wing moment coefficient (about 0.25 c), C_m
CMIM	m_α" in Tables 5 to 14; m_c" in Tables 15 to 23
CMRE	m_α' in Tables 5 to 14; m_c' in Tables 15 to 23
CP	mean pressure coefficient C_p
CPIM	imaginary component of oscillatory pressure coefficient, rad^{-1}. In Tables 5 to 14 it represents C_p"/α_0, in Tables 15 to 23 it represents C_p"/δ_0
CPRE	real component of oscillatory pressure coefficient, rad^{-1}. In Tables 5 to 14 it represents C_p'/α_0, in Tables 15 to 23 it represents C_p'/δ_0 . If k=0, then CPRE = $[C_p(+\alpha_o) - C_p(-\alpha_0)] / 2\alpha_0$ and CPRE = $[C_p(+\delta_o) - C_p(-\delta_0)] / 2\delta_0$ respectively.
DELTA	mean flap angle, δ_m deg
FREQ.	frequency, f, Hz
HARM	order of harmonic

k_α	oscillatory wing lift coefficient, $C_L/\pi\alpha_0$ rad^{-1}
k_c	oscillatory wing lift coefficient, $C_L/\pi\delta_0$ rad^{-1}
M	mean local Mach number, M_L
MACH	free-stream Mach number, M
m_α	oscillatory wing moment coefficient, -2 $C_m/\pi\alpha_0$, rad $^{-1}$
m_c	oscillatory wing moment coefficient, -2 $C_m/\pi\delta_0$, rad $^{-1}$
MEETRUNNR	run number
NCRE, NCIM	real and imaginary components of oscillatory flap moment coefficient, -2 $C_h/\pi\delta_0$, rad $^{-1}$
P0	total pressure, p_t , Pa
Q	dynamic pressure, q, Pa
RCRE, RCIM	real and imaginary components of oscillatory flap lift coefficient, $C_{Lf}/\pi\delta_0$
RE	Reynolds number based on wing chord, Re
RFREQ	reduced frequency, k = πfc/V
+	(suffix) upper side
-	(suffix) lower side
*	(superscript) critical value

Note: The oscillatory motions are defined as $\alpha = \alpha_0 \sin \omega t$ and $\delta = \delta_0 \sin \omega t$. The equation for a corresponding oscillatory pressure (including higher harmonics, if available) reads: $p(t) = p_m + p' \sin \omega t + p'' \cos \omega t + p_1' \sin 2\omega t + p_1'' \cos 2\omega t$ Similar expressions hold for the aerodynamic coefficients.

PRESENTATION OF DATA

The data which were presented in tables 1, 2, and 5 to 23 of the original AGARD R702 report for this test are supplied here in electronic form as ASCII files.

The file SET4TAB1.DAT contains the NLR7301 data given in table 1. The format is that the first record contains the number NU of upper surface points followed by NU records containing the Z value and X value for the points.After this the file contains the number NL of lower surface points followed by NL records containing the Z value and X value for the points.

The file SET4TAB2.DAT contains the model contour data given in table 2. The format is that the first record contains the number N of followed by N records containing Z, X upper surface, X lower surface for these N points.

The data which were presented in tables 5 to 23 are supplied here as a single ASCII data file SET4.UND in RUNAD format as defined in the introduction to chapter 3. The table numbers are used as the "run numbers" for data selection by the program RUNAD and the conditions corresponding to each table is given in table 4. Tables 6 and 16 are reproduced here as samples. Note that for the zero-frequency tests the values of CL, CM and CP given as "steady" apply for the airfoil with undeflected flap and the values given as "real parts of oscillatory" CL and CM and the DCP values apply to the deflected flap configuration.

FORMULARY

1 General Description of model

1.1	Designation	NLR 7301 (also NLR HT 7310810)
1.2	Type	Thick, aft-loaded, shock-free supercritical airfoil
1.3	Derivation	Airfoil designed by means of Boerstoel hodograph method
1.4	Additional remarks	Thickness/chord = 16.5%
1.5	References	-

2 Model Geometry

2.1	Planform	Two-dimensional airfoil
2.2	Aspect ratio	(2.33)

2.3	Leading edge sweep	0
2.4	Trailing edge sweep	0
2.5	Taper ratio	0
2.6	Twist	0
2.7	Wing centreline chord	0.18m
2.8	Span of model	0.42m
2.9	Area of planform	$0.0756m^2$
2.10	Location of reference sections and definition of profiles	See table 2
2.11	Lofting procedure between reference sections	NA
2.12	Form of wing-body junction	NA
2.13	Form of wing tip	NA
2.14	Control surface details	Flap with hinge at 75% chord, gap width 0.35mm
2.15	Additional remarks	Nose radius 0.05c Design condition - Potential flow hodograph theory M=0.721, C_L=0.595 Design pressure distribution (free transition, NLR Pilot Tunnel): M=0.747, C_L=0.455, see fig.9 "Shock-free" pressure distributions for configuration A shown in fig.2 and for configuration B in fig.6.
2.16	References	-

3 Wind Tunnel

3.1	Designation	NLR Pilot Tunnel
3.2	Type of tunnel	Continuous, closed circuit
3.3	Test section dimensions	Rectangular, see fig.10. Height 0.55m, width 0.42m.
3.4	Type of roof and floor	10% slotted top and bottom walls, separate top and bottom plenums
3.5	Type of side walls	Solid side walls
3.6	Ventilation geometry	See fig.10
3.7	Thickness of side wall boundary layer	Thickness 10% of test section semi-width, no special treatment
3.8	Thickness of boundary layers at roof and floor	Not measured. Probably comparable with side wall boundary layers
3.9	Method of measuring Mach number	Derived from static pressure measured upstream of model and from total pressure measured in settling chamber
3.10	Flow angularity	NA
3.11	Uniformity of Mach number over test section	See fig.11 (empty test section)
3.12	Sources and levels of noise or turbulence in empty tunnel	Turbulence/noise level, see fig.12
3.13	Tunnel resonances	No evidence
3.14	Additional remarks	For two-dimensionality of the flow see ref 3
3.15	References on tunnel	Ref 2

4 Model motion

4.1	General description	Hydraulic excitation at one side of the model. A pitching oscillation of airfoil B oscillation of trailing-edge flap
4.2	Natural frequencies and normal modes of model and support system	No interference with natural vibration modes

5 Test Conditions

5.1	Model chord/tunnel width	0.435
5.2	Model chord/tunnel height	0.323
5.3	Blockage	
5.4	Position of model in tunnel	
5.5	Range of Mach number	A: 0.5 to 0.8 B: 0.5 to 0.82
5.6	Range of tunnel total pressure	Atmospheric
5.7	Range of tunnel total temperature	$313 \pm 1^{\circ}$ K
5.8	Range of model steady or mean incidence	A: $\alpha_m = 0^{\circ}$ to 3° B: $\alpha_m = 0^{\circ}$ to 3°, $\delta_m = 0^{\circ}$
5.9	Definition of model incidence	Incidence datum line α=0 relates to the x-axis as used in tables 1 and 2. Datum line is parallel to test section centre line for $\alpha_m = 0$
5.10	Position of transition, if free	Part of the tests performed with natural transition, position of transition not measured
5.11	Position and type of trip, if transition fixed	A: strip of carborundum grains at 0.3 c B: strip of carborundum grains at 0.07 c or 0.3 c
5.12	Flow instabilities during tests	No evidence
5.13	Changes to mean shape of model due to steady aerodynamic load	Negligible
5.14	Additional remarks	-
5.15	References describing tests	A: ref.4

6 Measurements and Observations

6.1	Steady pressures for the mean conditions	Y
6.2	Steady pressures for small changes from the mean conditions	Y
6.3	Quasi-steady pressures	N
6.4	Unsteady pressures	Y
6.5	Steady section forces for the mean conditions by integration of pressures	Y
6.6	Steady section forces for small changes from the mean conditions by integration	Y
6.7	Quasi-steady section forces by integration	N
6.8	Unsteady section forces by integration	Y
6.9	Measurement of actual motion at points of model	Y
6.10	Observation or measurement of boundary layer properties	N
6.11	Visualisation of surface flow	N
6.12	Visualisation of shock wave movements	Y
6.13	Additional remarks	N

7 Instrumentation

7.1	Steady pressure	
	7.1.1 Position of orifices spanwise and chordwise	See 7.2.1
	7.1.2 Type of measuring system	See 7.2.3
7.2	Unsteady pressure	
	7.2.1 Position of orifices spanwise and	A: see fig.13 and 14

	chordwise	B: see fig.15 and 16
	7.2.2 Diameter of orifices	0.8mm
	7.2.3 Type of measuring system	A: 40 pressure tubes + 13 in situ pressure transducers B: 46 pressure tubes + 12 in situ pressure transducers
	7.2.4 Type of transducers	$\pm$7.5 psi Statham differential pressure transducers, and $\pm$5 psi Kulite miniature pressure transducers
	7.2.5 Principle and accuracy of calibration	Calibration uses transfer functions of pressure tubes, see ref.4, for accuracy see 9.10
7.3	Model motion	
	7.3.1 Method of measuring motion reference coordinate	A: with accelerometers, see fig.13 B: with accelerometers, see fig.15
	7.3.2 Method of determining spatial mode of motion	NA
	7.3.3 Accuracy of measured motion	See fig.10
7.4	Processing of unsteady measurements	
	7.4.1 Method of acquiring and processing measurements	See fig.17
	7.4.2 Type of analysis	A: signal analysis of TFA over 20 cycles for f=30, 80 Hz and 60 cycles for f=200 Hz B: signal length during TFA analysis was 1 sec
	7.4.3 Unsteady pressure quantities obtained and accuracies achieved	A: Fundamental harmonics B: Fundamental harmonics and occasionally second and third harmonics For accuracy see 9.10
	7.4.4 Method of integration to obtain forces	Trapezoidal rule
7.5	Additional remarks	-
7.6	References on techniques	A: ref 4 and 5 B: ref 6

8 Data presentation

8.1	Test cases for which data could be made available	A: see table 3 B: not available
8.2	Test cases for which data are included in this document	See table 4. Amplitude A: $\alpha_0 = 0.1°$ to $1.5°$ B: $\delta_0 = 0.1°$ to $2°$ Frequency A: f =0 to 80 Hz (k=0 to 0.26) B: f=0 to 200 Hz (k=0 to 0.65)
8.3	Steady pressures	Mean pressures for: A: tables 5 to 14 B: tables 15 to 23
8.4	Quasi-steady or steady perturbation pressures	Steady pressure derivatives for: A: tables 5, 8, 12 B: tables 15, 17, 19
8.5	Unsteady pressures	A: tables 6, 7, 9, 10, 11, 13, 14 B: tables 16, 18, 20 to 23
8.6	Steady forces or moments	See 8.3
8.7	Quasi-steady or unsteady perturbation forces	See 8.4
8.8	Unsteady forces and moments	See 8.5
8.9	Other forms in which data could be made available	NA
8.10	Reference giving other representations of data	NA

9 Comments on data

9.1	Accuracy	
9.1.1	Mach number	$\pm$0.002. No corrections made for Mach number non-uniformity
9.1.2	Steady incidence	$\pm$0.02°
9.1.3	Reduced frequency	$\pm$0.0005
9.1.4	Steady pressure coefficients	Not known
9.1.5	Steady pressure derivatives	Not applicable
9.1.6	Unsteady pressure coefficients	Not known
9.2	Sensitivity to small changes of parameter	No evidence
9.3	Non-linearities	Part of analysis of experimental results, see ref.4
9.4	Influence of tunnel total pressure	NA
9.5	Effects on data of uncertainty, or variation, in mode of model motion	NA
9.6	Wall interference corrections	No corrections included, but under steady conditions it is normal to make the following steady corrections to measurements made in this tunnel: $\Delta\alpha_m = -1.4\ C_L + 0.56\ (C_m + 0.25\ C_L)/\ (1-M^2)^{-1/2}$ (deg) ($\pm$15%) $\Delta C_L = -0.015\ C_L\ /\ (1-M^2)$, ($\pm$30%) $\Delta C_m = -0.25\ \Delta C_L$ ($\pm$30%)
9.7	Other relevant tests on same model	None
9.8	Relevant tests on other models of nominally the same shapes	See data set 5 of R702.
9.9	Any remarks relevant to comparison between experiment and theory	-
9.10	Additional remarks	No systematic investigations of separate accuracies have been performed. Accuracy of lift and moment coefficients is estimated to be 5 to 10 per cent in magnitude and 3 to 6 degrees in phase angle.
9.11	References on discussion of data	A: ref.4

10 Personal contact for further information

Evert G M Geurts
Department of Aerodynamics Engineering and Aeroelasticity
Phone: +31 20 5113455
Fax: +31 20 5113210
Email: geurts@nlr.nl

National Aerospace Laboratory NLR
Anthony Fokkerweg 2 P.O. Box 90502
NL 1059 CM Amsterdam NL 1006 BM Amsterdam
The Netherlands The Netherlands
Phone: +31 20 5113113
Fax: +31 20 5113210
Website: http://www.nlr.nl

11 List of references

1 T Barche c.s. Experimental data base for computer program assessment. AGARD-AR-138, 1979

2 J Zwaaneveld Principal data of the NLL Pilot Tunnel. NLL Report MP 185, 1959

3 H A Dambrink Investigation of the 2-dimensionality of the flow around a profile in the NLR 0.55x0.42m transonic wind tunnel. NLR Memorandum AC-72-018, 1972

4 H Tijdeman Investigations of the transonic flow around oscillating airfoils. NLR TR 77090 U, 1977

5 P H Fuykschot, L J M Joosten DYDRA - Data logger for dynamic measurements. NLR MP 69012 U, 1969

6 P H Fuykschot PHAROS, processor for harmonic analysis of the response of oscillating surfaces. NLR MP 77012 U, 1977

7 S R Bland AGARD Two-dimensional aeroelastic configurations. AGARD-AR-156, 1979

Table 1 Contour data of the NLR 7301 airfoil

The contour data is contained in the file SET4TAB1.DAT

Table 2

Actual contour data of the NLR 7301 airfoil (conf. B) (measured in mm) is contained in the file SET4TAB2.DAT

Note regarding Tables 1 and 2:

In Ref. 7 the contour coordinates have been transformed to unit chord. The model was designed to shape given by Table 1, but the trailing edge was cut off at x/c=1.0. The actual measured shape of the model is given in the table above.

Table 3

Test program for the NLR 7301 airfoil (conf.A)

Basic program: amplitude of oscillation: $\alpha_0 = 0.5°$
frequencies: 0, 10, and 80 Hz
transition strip at x/c=0.3

Incidence α_m degrees	Mach number										
	0.5	0.6	0.65	0.675	0.70	0.725	0.74	0.75	0.76	0.775	0.80
0	x				x			x			
0.85	x	x	x	x	x	x	x	x	x	x	x
1.50	x				x			x			
3.00	x	x	x	x	x	x		x			

Influence of amplitude and frequency, transition strip at x/c=0.3

Incidence α_m degrees	Amplitude α_0 degrees	Frequency Hz	Mach number		
			0.5	0.7	0.75
0.85	0.1, 0.25, 0.75, 1.0, 1.5	10, 80	x	x	x
3.00	0.1, 0.25, 0.75, 1.0	10, 80		x	
0.85	0.5, 1.0	10, 30, 60, 80	x	x	x
3.00	0.5, 1.0	10, 30, 60, 80		x	

Additional tests with natural transition

Incidence α_m degrees	Amplitude α_0 degrees	Frequency Hz	Mach number		
			0.5	0.7	0.75
0.85	0.5, 1.0	10	x	x	x
0.85	0.5, 0.75	80	x	x	x
3.00	0.5, 1.0	10		x	
3.00	0.5, 0.75	80		x	
0.85	0.5	30, 60	x	x	x

Table 4 Test cases for the NLR 7301 airfoil (confs A and B) included in this Data Set

Motion	Flow	CT case					Data Set									
		N_0	M	α_m	α_0,δ_0	k	Run no.	M	α_m	δ_m	α_0, δ_0	k	$Re*10^{-6}$	transition	Harm.	Table
Pitching about 0.4c (conf.A)	Subsonic	z1	0.500	0.40	0.5	0	12201	0.499	0.85		0.50	0	1.70	0.3c	1	5
		1	0.500	0.40	0.5	0.098	1601	0.499	0.85		0.55	0.098	1.70	0.3c	1	6
		2	0.500	0.40	0.5	0.262	1301	0.498	0.85		0.44	0.262	1.70	0.3c	1	7
	Transonic with shock	z2	0.700	2.00	0.5	0	14405	0.696	3.00		0.50	0	2.11	0.3c	1	8
		3	0.700	2.00	0.5	0.072	3805	0.696	3.00		0.42	0.072	2.11	0.3c	1	9
		4	0.700	2.00	1.0	0.072	3905	0.696	3.00		0.98	0.072	2.11	0.3c	1	10
		5	0.700	2.00	0.5	0.192	52705	0.695	3.00		0.55	0.192	2.12	0.3c	1	11
	Supercritical design	z3	0.721	-0.19	0.5	0	16908	0.744			0.50	0	2.22	free	1	12
		6	0.721	-0.19	0.5	0.068	9608	0.744	0.85		0.46	0.068	2.23	free	1	13
		7	0.721	-0.19	1.0	0.068	xxx									
		8*	0.721	-0.19	0.5	0.181	6708	0.744	0.85		0.61	0.181	2.22	free	1	14
		9	0.721	-0.19	0.5	0.453	xxx									
Flap rotation (conf B)	Subsonic	z4	0.500	0.40	1.0	0	250	0.503	0	0.02	0.95	0	1.69	0.07c	1	15
		10	0.500	0.40	1.0	0.098	253	0.502	0	0.02	0.97	0.098	1.69	0.07c	1	16
	Transonic with shock	z5	0.700	2.00	1.0	0	129	0.702	3.00	-0.08	0.95	0	2.14	0.3c	1	17
		11	0.700	2.00	1.0	0.071	120	0.701	3.00	0.03	0.97	0.071	2.14	0.3c	1	18
	Supercritical design	z6	0.721	-0.19	1.0	0	160	0.754	0.85	0.01	0.96	0	2.23	free	1	19
		12	0.721	-0.19	1.0	0.067	148-150	0.755	0.85	0.01	0.95	0.067	2.23	free	1,2,3	20-22
		13*	0.721	-0.19	1.0	0.181	xxx									
		14	0.721	-0.19	1.0	0.445	162	0.756	0.85	-0.01	0.90	0.445	2.23	free	1	23

Remarks on Table 4

Cases z1 to z6 are extra to the computational cases identified in Ref. 7. They correspond to zero-frequency (k=0) experimental data that are closely related to the CT cases for which k≠0. The asterisks denote Priority Cases. xxx denotes cases for which no measurements are included.

Note that the table numbers in the right hand column are used as the reference number in the SET4.UND data file.

Sample table for configuration A - Table 6

RUN 1601

M	.499	C2	.55	STAT.	QUASI-INSTAT.
ALPHA	.85	FREQ	30.		RE IM
P0	10398.	K	0.000	CL .311	1.481 -.170
RE	1.70E6			CM .069	-.028 .151
Q	1529.				

		UPPERSIDE				LOWERSIDE		
X/C	CP+	M-	CPRE+	CPIM+	CP-	M-	CPRE-	CPIM-
.01	-.070	.518	-10.560	2.296	.296	.417	6.804	-3.146
.05	-1.163	.776	-11.456	2.389	-.351	.586	7.090	-2.048
.10	-.846	.703	-8.108	1.833	-.373	.592	4.808	-1.920
.15	-.707	.672	-3.138	.552	-.383	.594	4.104	-1.096
.20	-.654	.659	-4.080	.853	-.400	.598	3.403	-.864
.25	-.633	.655	-3.339	.514	-.415	.602	2.854	-.738
.30	-.642	.657	-2.972	.213	-.413	.601	2.725	-.614
.35	-.599	.647	-2.920	.004	-.426	.604	2.671	.011
.40	-.594	.645	-2.415	.024	-.440	.608	2.356	.164
.45	-.582	.643	-2.089	-.054	-.440	.608	1.963	.091
.50	-.571	.640	-1.804	-.181	-.393	.597	1.688	.237
.55	-.562	.638	-1.398	-.139	-.297	.573	1.492	.238
.60	-.542	.633	-1.045	-.155	-.201	.550	1.089	.164
.65	-.494	.622	-.705	-.200	-.084	.520	.852	.296
.70	-.410	.602	-.412	-.227	.030	.491	.259	-.067
.75	-.307	.577	-.191	-.277	.130	.464	.547	.422
.80	-.195	.549	.054	-.279	.212	.441	.571	.457
.85	-.085	.522	.091	-.256	.269	.425	.562	.533
.90	.011	.497	-.090	-.152	.300	.416	.440	.431
.95	.086	.477	-.466	-.092	.302	.415	.250	.284

Sample table for configarion B - Table 16

FUNDAMENTAL FREQUENCY TEST DATA NLR 7301 WITH OSCILLATING FLAP

	UPPERSIDE				LOWERSIDE			
X/C	CP+	M-	CPRE+	CPIM+	CP-	M-	CPRE-	CPIM-
.010	.126	.469	-2.159	1.234	.069	.484	2.243	-1.519
.030	-.935	.728	-3.015	1.557	-.464	.618	2.675	-1.422
.050	-.867	.713	-.883	1.411	-.531	.634	.973	-1.323
.100	-.629	.658	-1.950	.987	-.472	.620	1.900	-.860
.150	-.570	.643	-1.384	.755	-.471	.620	1.389	-.839
.200	-.545	.638	-1.238	.629	-.474	.621	1.321	-.673
.250	-.534	.635	-1.237	.629	-.483	.623	1.201	-.568
.300	-.522	.632	-1.363	.483	-.488	.624	.976	-.584
.350	-.512	.630	-1.362	.484	-.488	.624	1.306	-.447
.400	-.509	.629	-1.290	.421	-.497	.626	1.419	-.439
.450	-.503	.628	-1.425	.411	-.483	.623	1.418	-.439
.500	-.501	.627	-1.551	.266	-.431	.610	1.521	-.320
.550	-.487	.624	-1.550	.266	-.328	.585	1.622	-.201
.600	-.470	.620	-1.820	.247	-.222	.559	1.776	-.024
.650	-.421	.608	-1.954	.239	-.107	.530	1.929	.152
.700	-.340	.588	-2.347	.078	.009	.500	1.970	.319
.725	-.283	.574	-2.416	.144	.057	.487	1.975	.205
.760	-.269	.571	-3.494	.072	.117	.471	2.123	.492
.775	-.233	.562	-2.728	-.215	.140	.465	1.788	.471
.800	-.172	.547	-1.711	-.213	.174	.455	1.565	.456
.850	-.067	.520	-.901	-.159	.228	.440	1.119	.429
.900	.022	.497	-.568	-.069	.261	.430	.955	.362
.950	.097	.476	-.425	-.194	.270	.428	.517	.225

TEST DATA		MODEL DATA			OVERALL DATA				
							STEADY	UNSTEADY	
								RE	IM
MEETRUNNR.	253	ALPHA	.00	DEG.					
MACH	.502	DELTA	.02	DEG.	NORMAL FORCE	CL	.172	.927	-.197
Q [PA]	15024	AMPL.	.97	DEG.	MOMENT(1/4C)	CM	.058	.418	.065
RE	1.69E6	FREQ.	30.0	HZ	FLAP FORCE	RC	.0625	.1705	.0376
HARM	1	RFREQ	.098		HINGE MOMENT	NC	.0059	.0255	.0077
IDENTNR.	10								

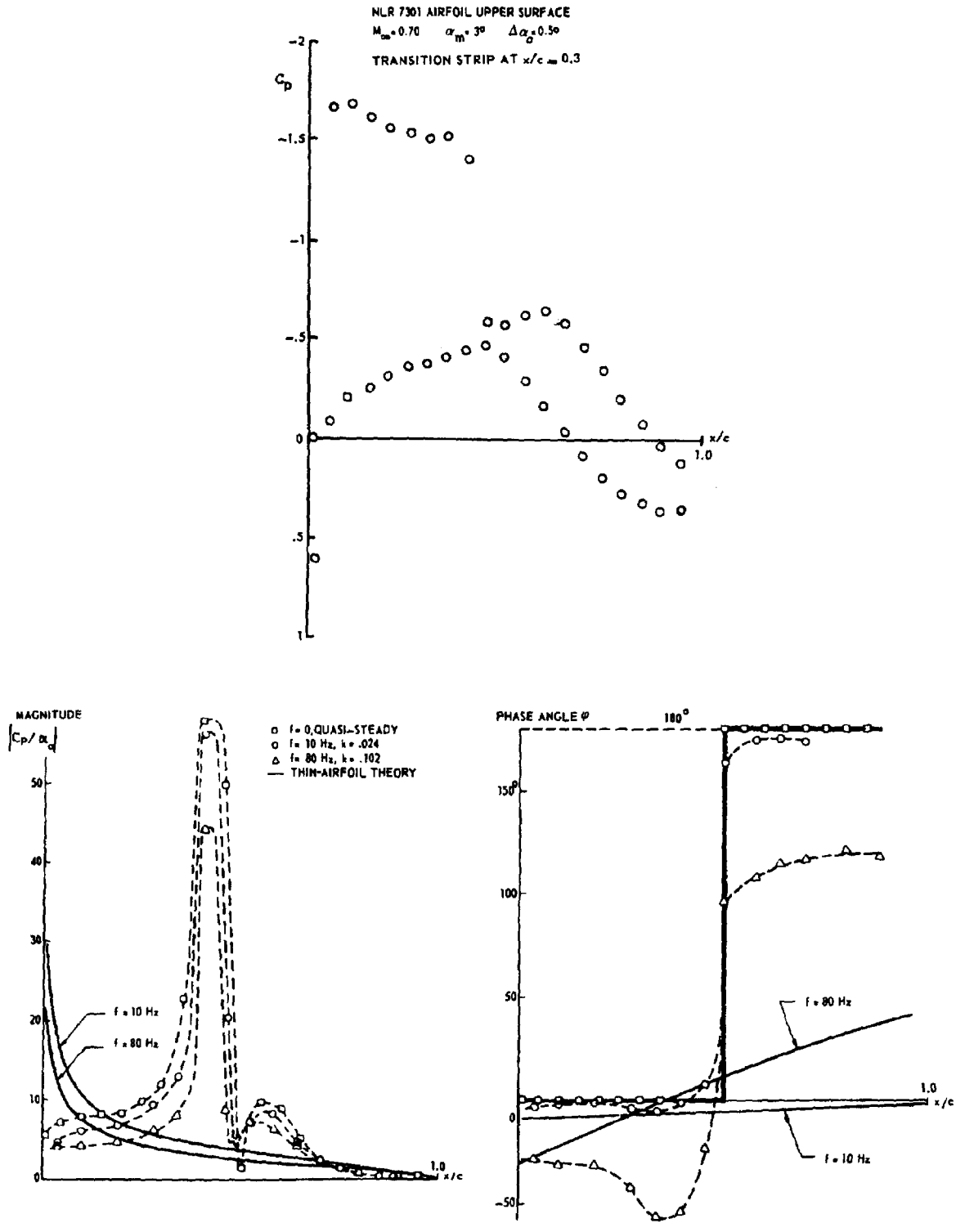

Fig. 1 Effect of shock wave on the unsteady pressure distributions; pitching oscillation

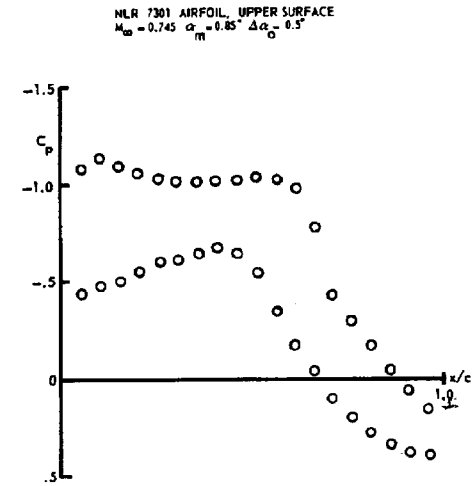

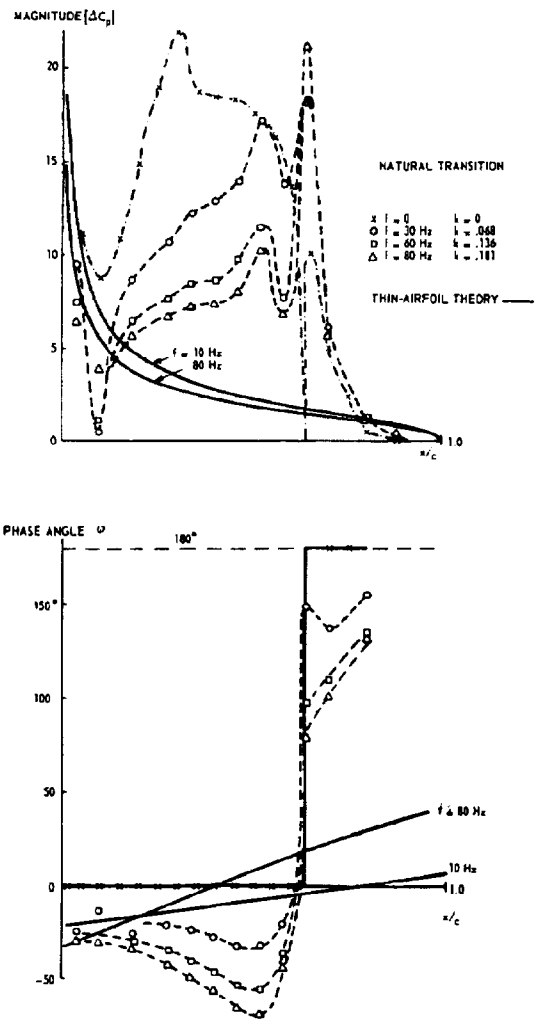

Fig. 2 Unsteady pressure distributions for the "shock-free" design point; pitching oscillation

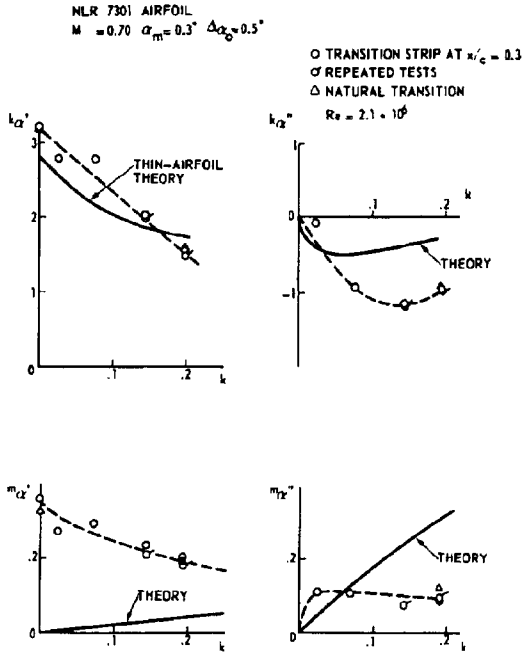

Fig. 3 Unsteady normal-force and moment coefficients as a function of frequency in transonic flow with a well-developed shock wave; pitching oscillation

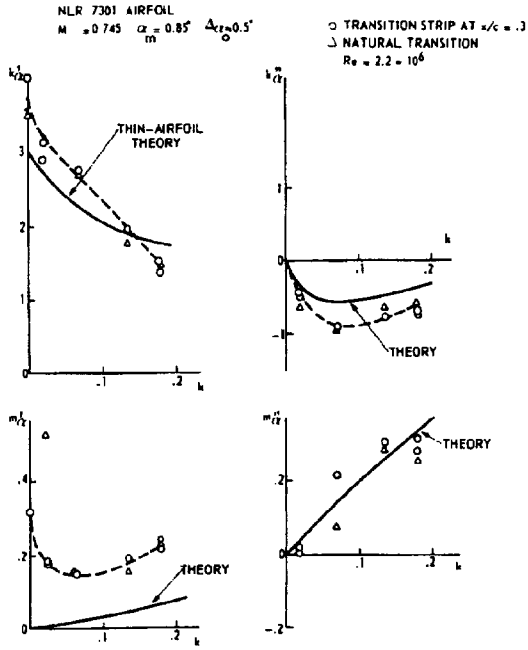

Fig. 4 Unsteady normal-force and moment coefficients as a function of frequency for the "shock-free" design point; pitching oscillation

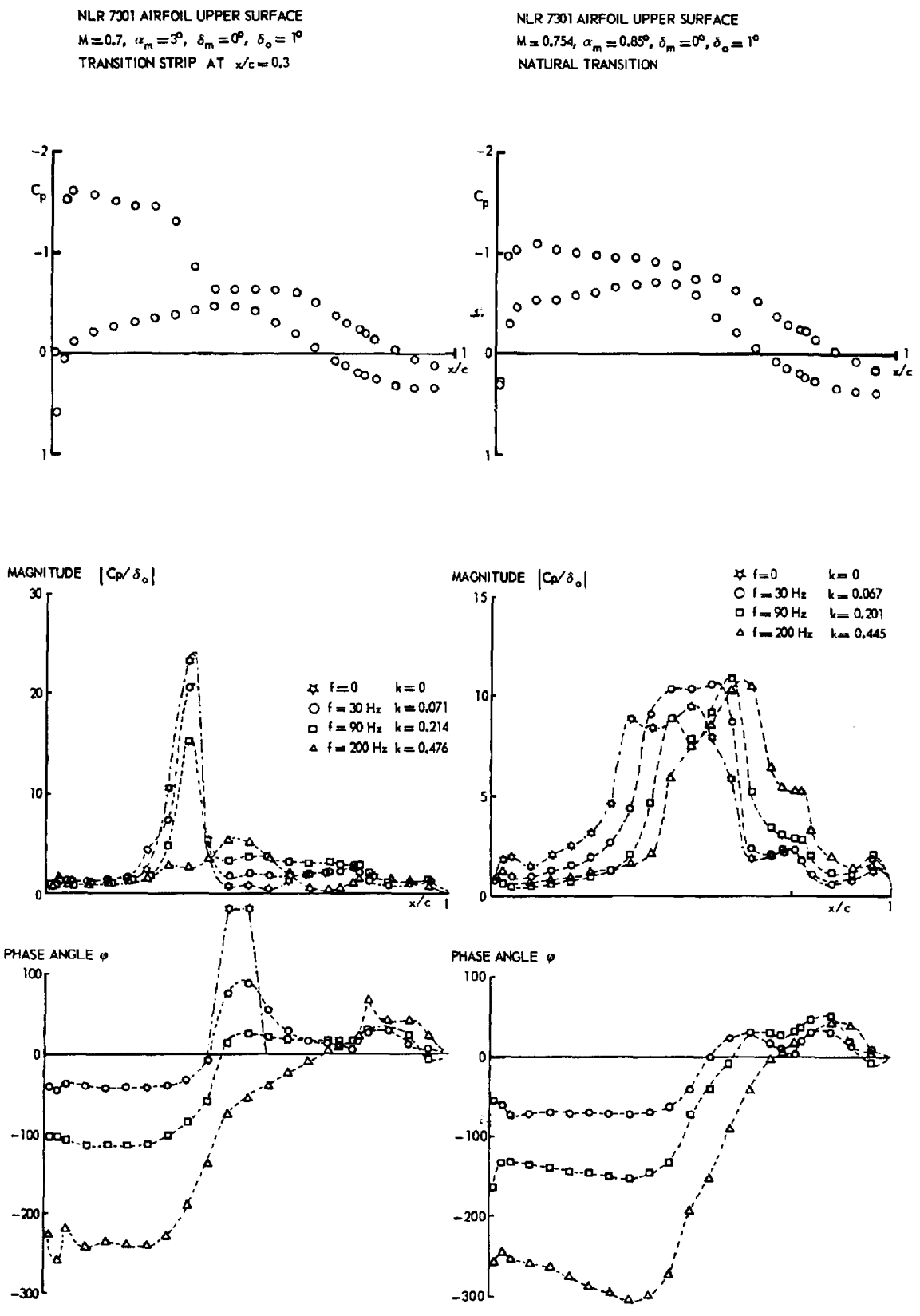

Fig. 5 Effect of shock wave on the unsteady pressure distributions; flap oscillation

Fig. 6 Unsteady pressure distributions for the "shock-free" design point; flap oscillation

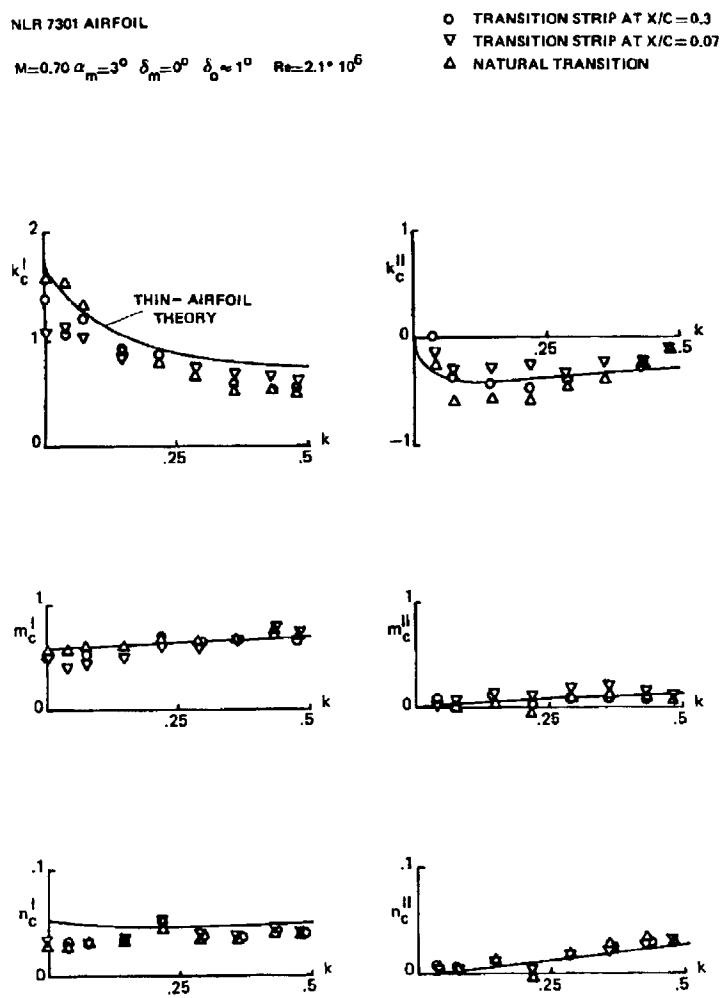

Fig. 7 Unsteady aerodynamic coefficients as functions of frequency in transonic flow with a well-developed shock wave; flap oscillation

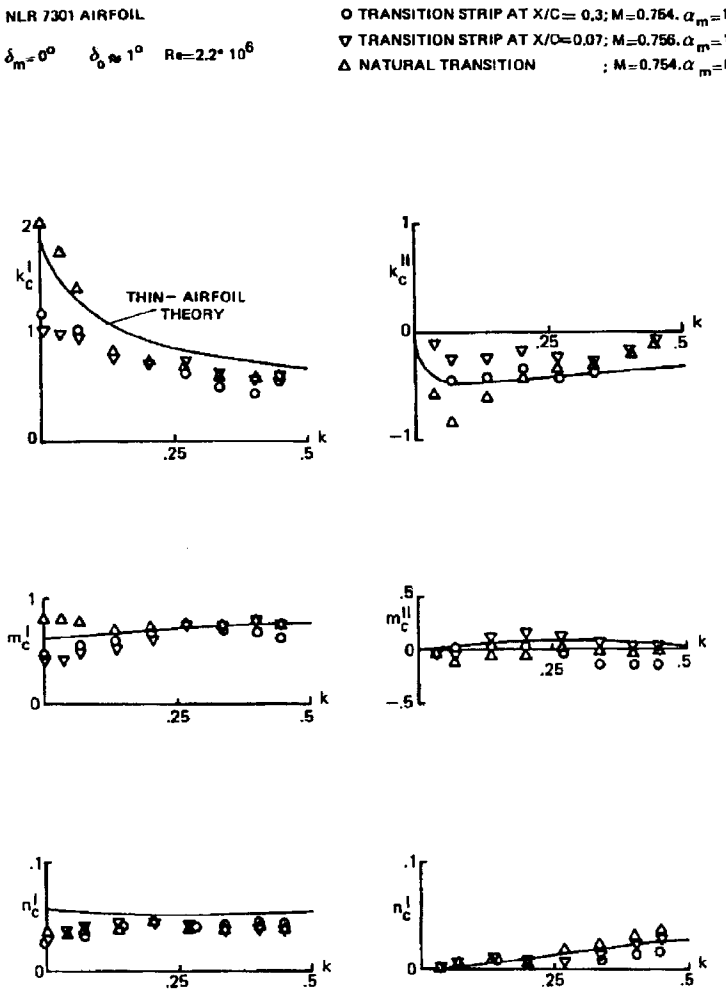

Fig. 8 Unsteady aerodynamic coefficients as functions of frequency for best "shock-free" steady flow; flap oscillation

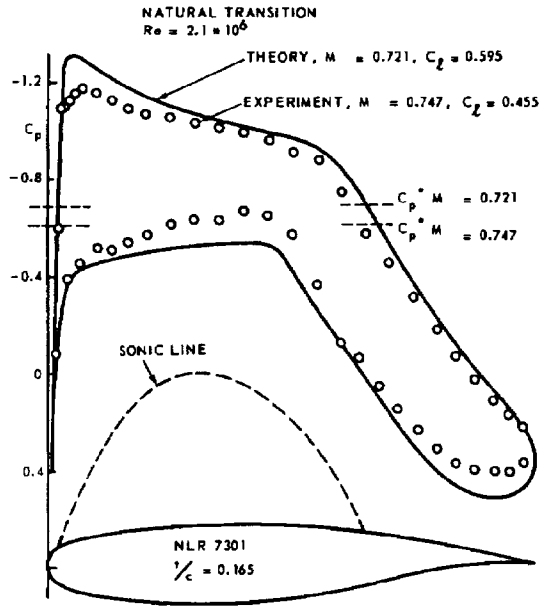

Fig. 9 Theoretical and experimental "shock-free" pressure distributions of the NLR 7301 airfoil (free transition)

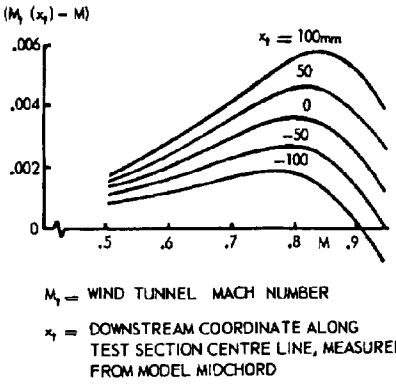

Fig. 11 Mach number distribution in NLR Pilot Tunnel test section

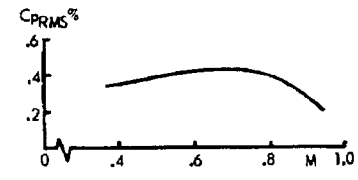

Fig. 12 Noise level in NLR Pilot Tunnel test section

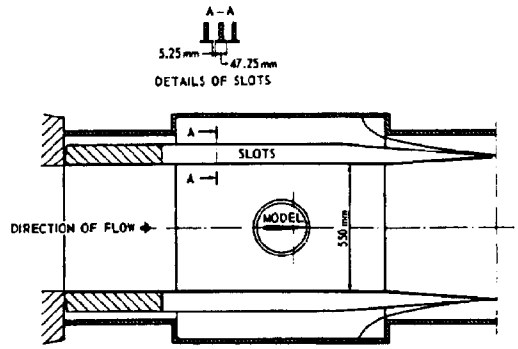

Fig. 10 Transonic test section of the NLR Pilot Tunnel

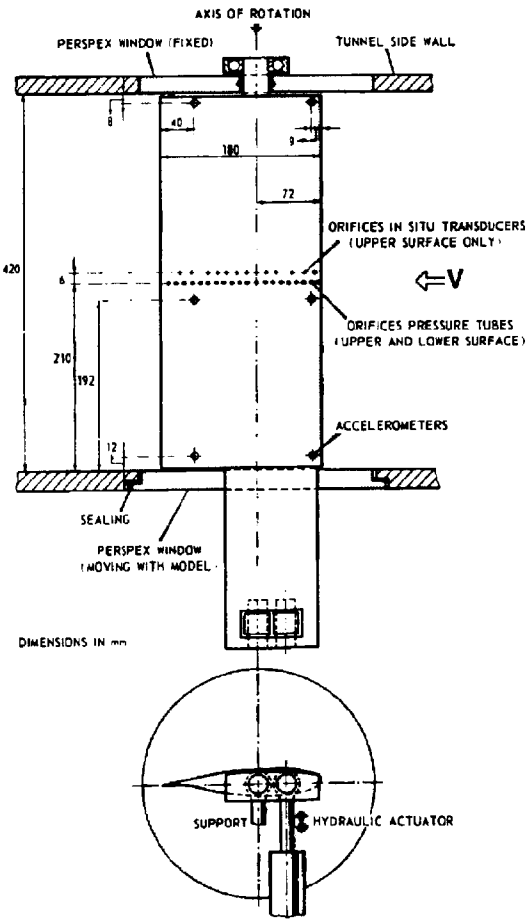

Fig. 13 Test set-up and instrumentation of the NLR 7301 airfoil (Conf. A)

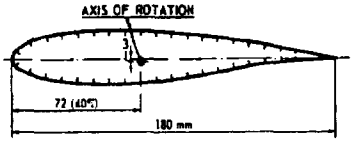

PRESSURE ORIFICES TUBING SYSTEM (BOTH UPPER AND LOWER SURFACE)				IN SITU TRANSDUCERS (UPPER SURFACE ONLY)			
No. 1	x/c = .01	No. 11	x/c = .50	No. 1	x/c = .04	No. 11	x/c = .70
2	.05	12	.55	2	.10	12	.80
3	.10	13	.60	3	.19	13	.88
4	.15	14	.65	4	.28		
5	.20	15	.70	5	.34		
6	.25	16	.75	6	.40		
7	.30	17	.80	7	.46		
8	.35	18	.85	8	.52		
9	.40	19	.90	9	.58		
10	.45	20	.95	10	.64		

Fig.14 Location of pressure orifices of the NLR 7301 airfoil (Conf. A)

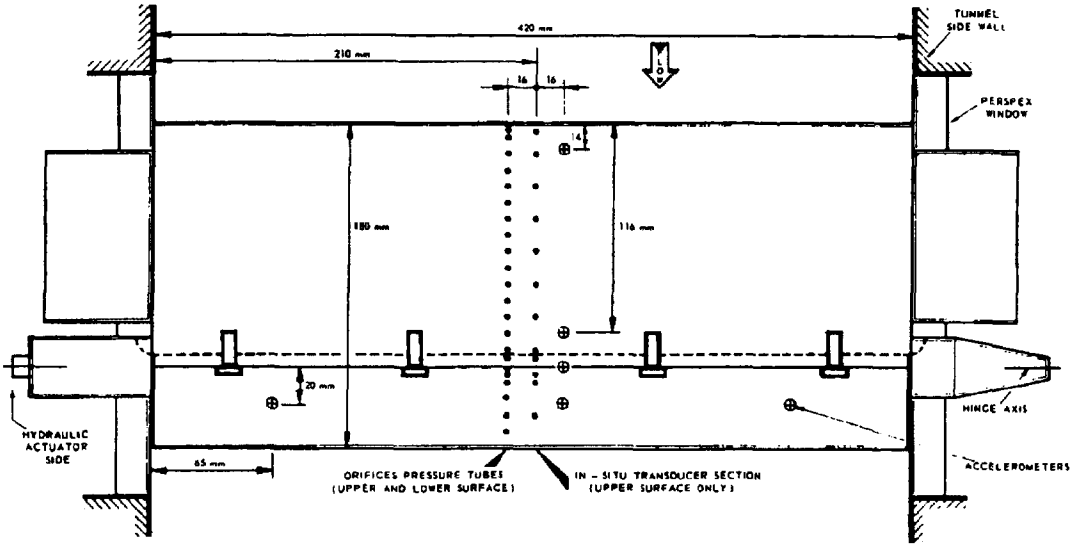

Fig.15 Test set-up and instrumentation of the NLR 7301 airfoil with control surface (Conf. B)

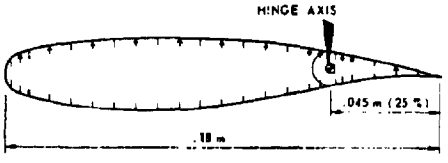

PRESSURE ORIFICES TUBING SYSTEM (both upper and lower surface)				IN SITU TRANSDUCERS (upper surface only)	
no. 1	x/c = .01	no. 13	x/c = .55	no. 1	x/c = .03
2	.03	14	.60	2	.10
3	.05	15	.65	3	.20
4	.10	16	.70	4	.30
5	.15	17	.725	5	.40
6	.20	18	.76	6	.50
7	.25	19	.775	7	.60
8	.30	20	.8	8	.70
9	.35	21	.85	9	.725
10	.40	22	.90	10	.775
11	.45	23	.95	11	.80
12	.50			12	.90

Fig.16 Location of pressure orifices of the NLR 7301 airfoil with control surface (Conf. B)

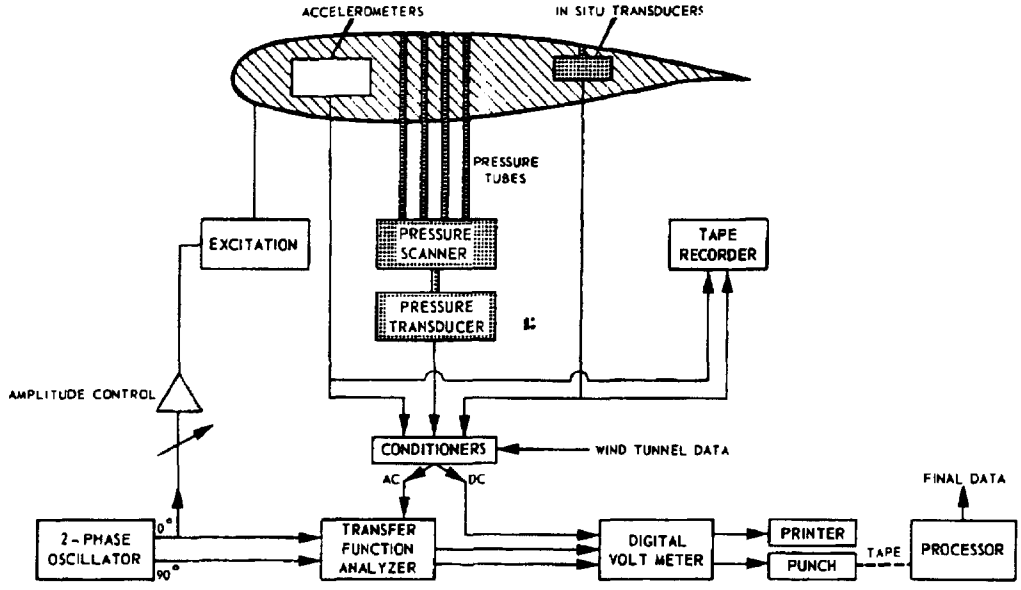

Fig. 17 Block diagram of measuring equipment (Conf. A). Similar equipment essentially for Conf. B